COMPDYN 2021
8th ECCOMAS Thematic Conference on
Computational Methods in Structural Dynamics and Earthquake Engineering
M. Papadrakakis, M. Fragiadakis (eds.)
Streamed from Athens, Greece, 27—30 June 2021

THE INFLUENCE OF IMPACT MODELLING ASSUMPTIONS ON THE DYNAMIC BEHAVIOUR OF FLEXIBLE ROCKING OSCILLATORS

Huanian Zhu[1], Manolis Chatzis[2], and Sinan Acikgoz[2]

[1]Phd Candidate, Department of Engineering Science, The University of Oxford
Parks Road, Oxford OX1 3PJ
e-mail: huanian.zhu@eng.ox.ac.uk

[2] Associate Professor, Department of Engineering Science, The University of Oxford
Parks Road, Oxford OX1 3PJ
e-mail: {manolis.chatzis, sinan.acikgoz}@eng.ox.ac.uk

Keywords: rocking, lateral flexibility, impact, analytical model.

Abstract. *For rigid rocking models, energy dissipation relies solely on impact. Consequently, the position of the impulse acting on the rocking body determines the magnitude of energy loss and strongly influences the subsequent dynamic response. This paper evaluates the corresponding influence of the location of the vertical impulse on the dynamic behaviour of flexible rocking oscillators. The dynamic behaviour of a rocking flexible oscillator is explored in this study with an impact model that parametrically considers the position of impulse. The influence of the position of impulse on the expected energy loss during impact, and on the overturning stability of the flexible rocking oscillator are then examined. It is shown that the energy loss at impact reduces and the potential for overturning instability increases, for impulses located at increasing distances from the future rocking corner.*

1 INTRODUCTION

The rocking problem of a rigid body was first systematically studied by Housner [1] with the inverted pendulum model (IPM). Several idealisations were made: the rocking body and the support medium are rigid; sliding and complete separation of the body from the support are prevented; the motion is restricted to be planar; dissipation of energy depends exclusively on impact. The impulse forces at impact were assumed to act on the future rocking corner. Consequently, the resulting energy loss can be described as a function of the geometry of the rigid body, and is often quantified with a coefficient of restitution parameter.

The coefficient of restitution arising from the assumption of impulses being applied at the future rocking corner was found to overestimate the energy dissipation during impact by various experimental investigations [2, 3, 4]. Modified values for the coefficient of restitution were used in numerical simulations to achieve a better fit with experimental data. A similar approach was followed for flexible oscillators by Acikgoz et al. [5, 6]. Kalliontzis et al. [7] modified coefficient of restitution in a different way. A new width of the body was adopted by noting the varying location of the instantaneous rocking corner of the rigid rocking body. The coefficient of restitution was obtained by conserving angular momentum with the new future rocking corner. Furthermore, coefficient of restitution was noticed to be velocity-dependent [3, 4, 8].

However, Shenton and Jones [9] noted that conserving angular momentum with a point other than the future rocking corner is not a necessity dictated by mechanics: they hinted the ratio of the impulse at the future rocking corner and the one at the previous rocking corner can be a non-zero value (though a ratio of zero was adopted). Chatzis et al. [8] further extended this observation and quantified the influence of the location of the vertical impulse on the overturning stability of rigid bodies: the future rocking corner was determined to be the least conservative location. These results have later been extended to stacked rocking bodies [10].

The aforementioned publications show that the modelling of coefficient of restitution is of significant importance to model the dynamics of rigid rocking bodies. This paper is devoted to exploring the influence of modelling the coefficient of restitution for the flexible rocking oscillator. In particular, it investigates how the coefficient of restitution is influenced by the position of impulses, and how coefficient of restitution further influences the rocking response.

2 ANALYTICAL MODEL

The model is illustrated in Figure 1(a). There are two masses: the top one is a concentrated mass m with negligible rotational mass moment of inertia at point P; the bottom one is a concentrated mass m_A with mass moment of inertia I_A at point A. The bottom mass takes the form of a rigid 'U' structure with a centroid at A; while the top mass is connected to the 'U' structure by a spring (with stiffness, k) and a viscous damper (with damping coefficient, c).

The body is symmetrical about a central vertical axis. The half width of the base is denoted by b. The slenderness of the bottom mass, centroid, and top mass are given by α_A, α_{cg}, and α. The height of the corresponding positions are h_A, h_{cg}, and h while their distances to either base corner are given by R_A, R_{cg}, and R, where cg refers to the centre of gravity.

There are three motion phases in this model: full contact phase, rocking around the left corner o', and rocking around the right corner o. The mechanical constraint for each phase is illustrated in Figure 1(b)-1(d). Two degrees of freedom exist: the rotation of the body θ and the lateral displacement u of the top mass. The system is subjected to horizontal ground accelerations $\ddot{x}_g$. Based on the mechanical constraints and excitations, the equations of motion for each phase is derived using Newton's law. They are similar to the ones proposed by Acikgoz

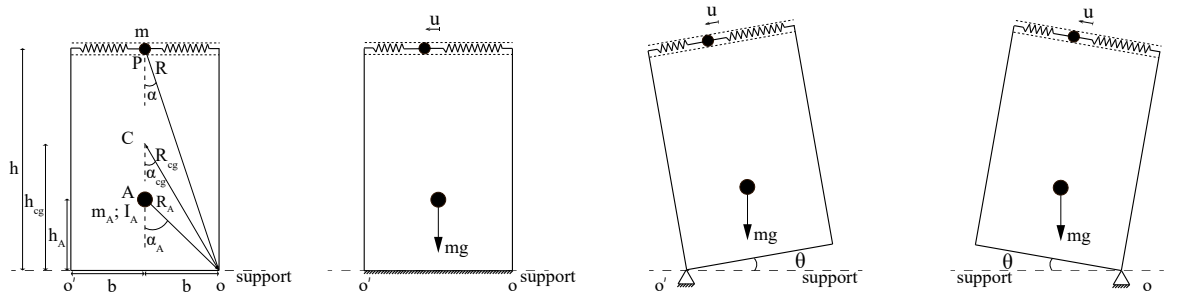

(a) Rocking model (b) Full contact phase (c) Rocking around o' (d) Rocking around o

Figure 1: Rocking model and phases.

and DeJong [11], with the difference of the bottom mass at non-zero height.

After obtaining the equations of motion, phase transition rules are defined. There are two types of transition: uplift and impact, with the former indicating a transition from full contact phase to a rocking phase, and the latter a transition from a rocking phase to another rocking phase or to a full contact phase.

During full contact, the reaction forces from the support medium move along the base of the body. Uplift happens when the position of the vertical reaction force coincides with one of the corners of the base. Uplift involves a smooth transition between two phases of motion. In contrast, impact involves impulsive forces and features a non-smooth transition. The horizontal impulse experienced by the top mass is zero, as the spring and damper cannot transmit impulsive forces over an infinitesimally small duration impact. Using this information and noting that angular momentum is conserved around the locus of the impulsive force (located at a distance λb from the future rocking corner) allows the calculation of the post-impact angular velocity $\dot{\theta}^+$. The following equation expresses the coefficient of restitution e which relates pre-impact and post-impact angular velocities (i.e. $\dot{\theta}^+ = e\dot{\theta}^-$) for the body transitioning from a pure-rocking phase to another pure-rocking phase:

$$e = \frac{I_A + m_A h_A^2 + mu(\mp b + u) + b(1-\lambda)(-m_A b - mb \pm mu)}{I_A + m_A h_A^2 + mu(\pm b + u) + b(1-\lambda)(+m_A b + mb \pm mu)} \tag{1}$$

Here, the upper sign refers to transitions from rocking around the left corner to rocking around the right corner, and the lower sign refers to vice versa. If e is positive, a new rocking phases follows. A negative value is mechanically inadmissible; in this case, a transition to full contact phase is assumed. For this to occur, $e = 0$ and this implies that λ attains a specific value λ_0. In the absence of any horizontal impulsive forces applied to the top mass, its post-impact velocity is determined by the conservation of horizontal momentum.

3 INFLUENCE OF IMPULSE POSITION ON ROCKING BEHAVIOUR

3.1 Dimensional analysis

To obtain the effects of the position of impulses on rocking behaviour systematically, dimensional analysis is employed. Single cycle sine and cosine pulses are used as excitations:

$$\ddot{x}_g = \begin{cases} A\mathbf{P}(\omega t) & t \leq 2\pi/\omega \\ 0 & t > 2\pi/\omega \end{cases} \tag{2}$$

where $\mathbf{P}$ denotes either $\sin$ or $\cos$; A and ω denote the amplitude and frequency of the pulse.

Under the excitations shown in Equation (2), the response of the rocking oscillator can be characterised by Equation (3).

$$(u, \theta) = f(\omega_n, \zeta_n, \alpha, \alpha_A, \omega, A, t, m, m_A, I_A, g, b, \lambda) \tag{3}$$

With 13 parameters and 3 fundamental dimensions involved, the two non-dimensional response parameters can be expressed by $13 - 3 = 10$ non-dimensional parameters according to Buckingham's Π theorem [12]. The chosen three repeating parameters are: p, g and m, while the Π groups are shown in Table 1. Note p is the frequency for rocking ($p = \sqrt{(m + m_A)gR_{cg}/(I_A + m_A R_A^2 + mR^2)}$). Thus, the dimensionless response parameters u/u_{cr} and θ/α_{cg} can be obtained by Equation (4). u_{cr} is a displacement used to nondimensionalise lateral displacement, which corresponds to the critical lateral displacement when an undamped body with a zero bottom mass height uplifts ($u_{cr} = \pm\frac{(m_A/m+1)gb}{\omega_n^2 h}$).

Table 1: Π groups

Π groups	Π_1	Π_2	Π_3	Π_4	Π_5	Π_6	Π_7	Π_8	Π_9	Π_{10}
Quantity	ω_n/p	ζ_n	α_{cg}	α_A	ω/p	$A/(g\tan\alpha_{cg})$	pt	m_A/m	$I_A/(m_A R_A^2)$	λ

$$(u/u_{cr}, \theta/\alpha_{cg}) = f(\omega_n/p, \zeta_n, \alpha_{cg}, \alpha_A, \omega/p, A/(g\tan\alpha_{cg}), pt, m_A/m, I_A/(m_A R_A^2), \lambda) \tag{4}$$

3.2 Coefficient of restitution

The influence of the position of the vertical impulse, as expressed through the value of λ, on the coefficient of restitution can be estimated by evaluating Equation (1) numerically for a chosen rocking body. After defining the Π groups, a stocky but laterally flexible body is chosen to investigate the relationship between the coefficient of restitution, the position of the impulse and lateral displacement of the top mass at the moment of impact. The parameters chosen for the rocking body are given in Table 2. The relationship between e, λ and u/u_{cr} is illustrated in Figure 2 for a range of plausible values.

Table 2: Simulation parameters for investigation of coefficient of restitution

	Π_1	Π_2	Π_3	Π_4	Π_8	Π_9	Π_{10}
Figure 2	2.43	0.05	0.35	0.6	0.47	0.56	$[0, 1]$

Figure 2(a) shows that e is monotonically increasing with respect to λ. This can be confirmed to be true for all flexible rocking bodies. The partial derivative of e with respect to λ is shown in Equation (5) and is always positive. Thus, the increasing trend is confirmed. Chatzis et al. [8] established that the increase of λ within the expected physical bounds $[0, 2]$ leads to an increased coefficient of restitution for rigid rocking bodies. It is shown the trend is the same for flexible bodies.

$$\frac{\partial e}{\partial \lambda} = \frac{2(m + m_A)b^2(I_A + m_A h_A^2) + 2mm_A b^2 u^2}{[I_A + m_A h_A^2 + mu(\pm b + u) + b(1 - \lambda)(+m_A b + mb \pm mu)]^2} \tag{5}$$

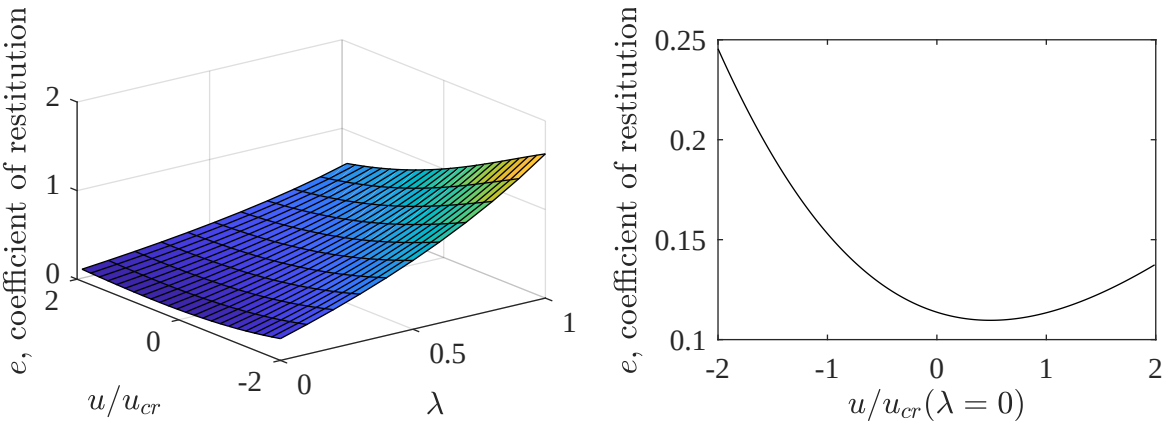

(a) 3D illustration (b) 2D illustration

Figure 2: Illustration of the relation between e, λ and u/u_{cr}.

Figure 2(a) indicates the noteworthy influence of lateral deformations u/u_{cr} on the coefficient of restitution e; while Figure 2(b) further investigates this relationship for an impulsive force locus at the future rocking corner, i.e. when $\lambda = 0$. Coefficient of restitution is clearly not a monotonic function of lateral deformation according to Figure 2(b). The lateral displacement u at impact, can reduce or increase the coefficient of restitution depending on its sign and magnitude.

For the example given in Figure 2, e is greater than 1 in some cases (e.g. $\lambda = 1$, $u/u_{cr} = -2$). However, different from the rigid body scenario, an e greater than 1 does not necessarily mean gaining energy during impact. Similarly, an e smaller than 1 can still lead to increase of energy. Furthermore, e with $\lambda = 0$, $u/u_{cr} = 0$ is much smaller than Housner's coefficient of restitution. This mainly reflects the effect of the absence of horizontal impulse applied at the top mass.

3.3 Stability analysis

A slender body is chosen to examine the influence of the impulse locus on overturning instability. The parameters are presented in Table 3. In the experiment by Espinosa [13], it is noticed $\lambda = 0.3$ is a reasonable value for the specific flat-base steel body placed on a sufficiently-stiff rubber mat. According to this, only three values of λ around 0.3 are included $(0, 0.2, 0.4)$ in the following simulations. Figure 3 shows the stability diagram of a stiffer body; while Figure 4 illustrates that of a more flexible body. For both bodies, a sine and a cosine pulse excitation is applied separately. Each point on the diagram corresponds to the result under a pulse with a specific nondimensional frequency (horizontal axis) and nondimensional amplitude (vertical axis). Three types of results are involved as indicated in Figure 3(a) (annotations are omitted in other figures as the location of different types of results are similar): mode 1 failure (overturning with one or more impacts), mode 2 failure (overturning without impact), safe case (no overturning). It can be seen from all the figures that an increase in λ leads to an expansion of mode 1 failure area.

Table 3: Simulation parameters for stability analysis

	Π_1	Π_2	Π_3	Π_4	Π_5	Π_6	Π_8	Π_9	Π_{10}
Figure 3(a)	2.43	0.05	0.15	0.28	$[0, 6]$	$[0, 8]$	0.47	0.56	$0, 0.2, 0.4$
Figure 3(b)	2.43	0.05	0.15	0.28	$[0, 6]$	$[0, 8]$	0.47	0.56	$0, 0.2, 0.4$
Figure 4(a)	9.82	0.05	0.15	0.28	$[0, 12]$	$[0, 24]$	0.47	0.56	$0, 0.2, 0.4$
Figure 4(b)	9.82	0.05	0.15	0.28	$[0, 6]$	$[0, 10]$	0.47	0.56	$0, 0.2, 0.4$

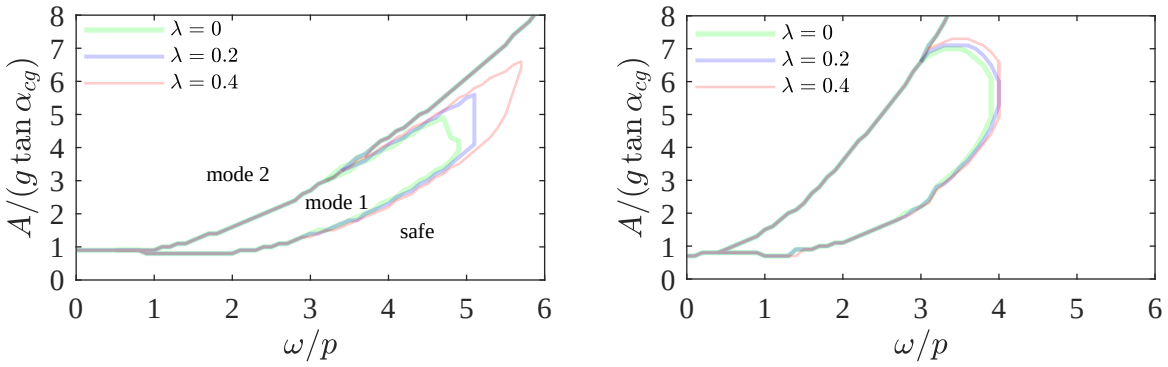

(a) Sine pulse (b) Cosine pulse

Figure 3: Effects of position of impulse on stability (flexible case).

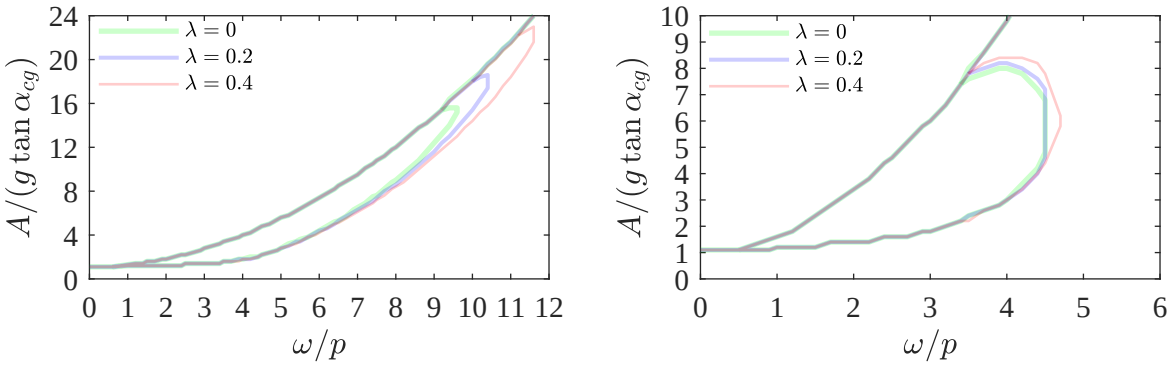

(a) Sine pulse (b) Cosine pulse

Figure 4: Effects of position of impulse on stability (stiff case).

The stability of the flexible rocking bodies is less sensitive to the change of λ under cosine pulse excitations. The trends are similar in Figures 3 and 4, indicating that the influence of λ on the stiff and flexible oscillators are qualitatively similar.

The increasing λ leads to more instances of overturning for the investigated flexible bodies, similar to the results obtained for rigid bodies [8]. In the rigid case, a reduced dissipation of energy can be predicted by the increase of λ since it directly determines energy loss. However, both rotational motion and lateral motion need to be considered to estimate energy loss at impact for the flexible body. Thus, a numerical example is chosen to demonstrate the total energy

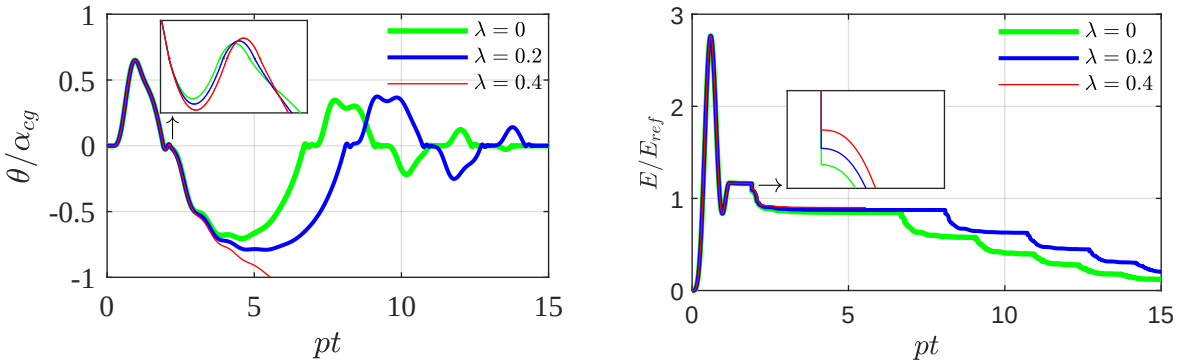

(a) Sine pulse

(b) Sine pulse

Figure 5: Time history example.

dissipation. The investigated rocking body is identical to the one shown in Figure 3(a), and its properties are provided in Table 3. The excitation that was considered is a sinusoidal pulse with $\omega/p = 5.3$ and $A/(g\tan(\alpha_{cg})) = 5$.

Figure 5(a)-5(b) show the time histories for rocking angle and total energy, which are all in normalised forms. Note that E_{ref} is the potential energy difference between the unstable and stable equilibrium points of a rigid body with a similar geometry [11]. It can be seen from the inset figure in Figure 5(b) that less energy was dissipated for larger λ, which leads to failure of the rocking body for $\lambda = 0.4$.

To generalise this result further, the total energy dissipation is investigated analytically. The following equation (6) shows the dissipated energy during impact (E_d); while the following equation (7) shows the partial derivative of E_d with respect to e, which is always negative for $e > 0$. Therefore, the dissipated energy is a monotonically decreasing function of e. Since a greater λ invariably leads to a greater e, the dissipated energy also decreases with the rise of λ. Therefore, it is reasonable to postulate that an increase in λ is likely to increase the risk of overturning for most types of excitations.

Nonetheless, due to the coupling between u and θ, it is possible for the rocking body to go directly from rocking into full contact [11]. The energy based considerations above do not account for this behaviour.

$$E_d = -\frac{1}{2}(I_A + m_A R_A^2 + mb^2 + mu^2)(e^2 - 1)(\dot{\theta}^-)^2 \mp mbu(e^2 + 1)(\dot{\theta}^-)^2 \tag{6}$$

$$\frac{\partial E_d}{\partial e} = -[I_A + m_A R_A^2 + m(b \pm u)^2]e(\dot{\theta}^-)^2 \tag{7}$$

It is also possible that a chosen value of λ may lead to an overall increase of the energy of the system during impact. Such values need to be avoided as the system would be gaining energy during impact. Similarly to [10], it is possible for this to happen for values of λ smaller than unity.

4 CONCLUSIONS

- A flexible rocking model and an impact model parametrising the location of the vertical impulse during impact is introduced.

- The effect of the position of the impulse on the coefficient of restitution is analytically and numerically examined, through studying the effect of changing the parameter λ.
- As the vertical impulse moves away from the future rocking corner, less energy is dissipated during impact. This is likely to lead to a higher risk of overturning instability.

REFERENCES

[1] G.W. Housner, The behavior of inverted pendulum structures during earthquakes. *Bulletin of the seismological society of America*, **53**, 403–417 1963.

[2] M. Aslam, W.G. Godden, D.T. Scalise, Earthquake rocking response of rigid bodies. *Journal of the Structural Division*, **106**, 377-392, 1980.

[3] Q. Ma, The mechanics of rocking structures subjected to ground motion. PhD diss., ResearchSpace@ Auckland, 2010.

[4] M.A. ElGawady, Q. Ma, J.W. Butterworth, J. Ingham, Effects of interface material on the performance of free rocking blocks. *Earthquake Engineering & Structural Dynamics*, **40**, 375-392, 2011.

[5] S. Acikgoz, Q. Ma, A. Palermo, M.J. DeJong, Experimental identification of the dynamic characteristics of a flexible rocking structure. *Journal of Earthquake Engineering*, **20**, 1199-1221, 2016.

[6] S. Acikgoz, M.J. DeJong, Analytical modelling of multi-mass flexible rocking structures. *Earthquake engineering & structural dynamics*, **45**, 2103-2122, 2016.

[7] D. Kalliontzis, S. Sritharan, A. Schultz, Improved coefficient of restitution estimation for free rocking members. *Journal of Structural Engineering* **142**, 06016002, 2016.

[8] M.N. Chatzis, M.G. Espinosa, A. Smyth, Examining the energy loss in the inverted pendulum model for rocking bodies. *Journal of Engineering Mechanics*, **143**, 04017013, 2017.

[9] H.W. Shenton III, N.P. Jones, Base excitation of rigid bodies. I: Formulation. *Journal of Engineering Mechanics* **117**, 2286-2306, 1991.

[10] M.N. Chatzis, M.G. Espinosa, C. Needham, M. S. Williams, Energy loss in systems of stacked rocking bodies. *Journal of Engineering Mechanics* **144**, 04018044, 2018.

[11] S. Acikgoz, M.J. DeJong, The interaction of elasticity and rocking in flexible structures allowed to uplift. *Earthquake Engineering & Structural Dynamics*, **41**, 2177–2194, 2012.

[12] E. Buckingham, On physically similar systems; illustrations of the use of dimensional equations. *Physical review*, **4**, 345, 1914.

[13] M.G. Espinosa, Risk estimation of rocking components subjected to ground motions. PhD diss., University of Oxford, 2018.